Laboratory Determination of Particle Deposition Uniformity on Filters Collected Using Federal Reference Method Samplers

Prepared by

Robert Vanderpool and Surender Kaushik

Office of Research and Development
National Exposure Research Laboratory
U.S. Environmental Protection Agency
Research Triangle Park, NC 27711

and

Marc Houyoux

Office of Air and Radiation
U.S. Environmental Protection Agency
Research Triangle Park, NC 27711

October 7, 2008

ABSTRACT

This report summarizes results of a study conducted by EPA's Office of Research and Development to determine the spatial uniformity of particles collected on FRM filters. These tests have relevance regarding the Agency's proposed use of EDXRF analysis for filters collected using PM_{10c} FRM samplers. The qualitative component of these tests involved stereoscopic examination of filters collected during field sampling as well as examination of filters collected in the laboratory using calibration aerosols in the 0.035 micrometer to 12.5 micrometer size range. The quantitative component of these tests was designed to determine the accuracy of using centrally located EDXRF spot sizes of 10 mm and 20 mm diameter to estimate the overall mass concentration of particles deposited over the entire filter surface. For purposes of comparison, these laboratory tests included uniformity measurements of filters collected with a $PM_{2.5}$ FRM sampler and a total filter sampler.

Examination of field collected filters confirmed previous reports of a thin deposition band at the extreme outside edge of the Teflon filter's collection area. This deposition band averaged approximately 0.5 mm in width and visually appeared to be of higher concentration than that of the remainder of the filter. Formation of the band occurred in the $PM_{2.5}$ FRM and the total sampler, as well as in the PM_{10c} sampler. Laboratory tests revealed that this deposition pattern results from non-uniform airflow at the outside edge of the FRM's Teflon filter due to the geometry of the filter membrane and its polypropylene support ring. Tests also revealed that the location and width of the deposition band depends upon the degree of concentricity of the filter cassette, the filter, and the backing screen during the cassette's assembly. Within the range of particle sizes tested, the formation and appearance of the outer deposition band was independent of particle diameter. Based on the observed width of the deposition band and the filter's total deposition area, the band comprises only approximately 5% of the filter's deposition area.

Quantitative tests revealed that formation of the outer deposition band apparently did not adversely affect the ability of a centrally located spot to estimate the filter's actual aerosol mass. Defining an accuracy ratio for a perfectly uniform deposition pattern as equal to 1.000, the ability of 10 mm and 20 mm punches to accurately estimate the filter's actual mass concentration was determined for each sampler. For a punch diameter of 10 mm, accuracy ratios were determined to be 0.981, 0.994, and 0.982 for the $PM_{2.5}$, PM_{10c}, and total filter samplers, respectively. For a punch diameter of 20 mm, accuracy ratios of 0.972, 0.993, and 0.985 were measured for the $PM_{2.5}$, PM_{10c}, and total filter samplers, respectively. Tests results also indicated no difference in deposition uniformity for particles generated in the 0.035 micrometer to 12.5 micrometer size range. Relevant to the proposed revisions to the Pb NAAQS, it can thus be concluded that any non-uniformity of particle deposition on PM_{10c} filters will represent a small fraction of the overall uncertainty in ambient Pb concentration measurement.

BACKGROUND

The proposed revisions to the NAAQS for Pb involves the use of energy dispersive x-ray fluorescence (EDXRF) to analyze filter samples collected using a PM_{10c} FRM sampler. Because EDXRF analysis only examines a fraction of the filter's deposition area, biases will exist in Pb concentration measurement if significant non-uniform spatial deposition is inherent to the collection method. To address this uncertainty, EPA's Office of Research and Development (ORD) conducted a focused study involving discussions with laboratory personnel responsible for gravimetric and EDXRF analysis of FRM filters, and qualitative and quantitative tests conducted in the laboratory under controlled conditions. ORD's qualitative tests involved stereoscopic examination of ambient aerosol samples collected during field sampling as well as examination of deposits obtained during sampling of laboratory generated aerosols. Quantitative tests were designed to determine the accuracy of using centrally located EDXRF spot sizes of 10 mm and 20 mm diameter to estimate the overall mass concentration of particles deposited over the entire filter surface. In the laboratory, hollow steel punches were used to remove representative filter sections for subsequent fluorometric quantitation of deposited solid ammonium fluorescein particles. These tests involved calibration aerosols generated in six discrete sizes from 0.035 micrometer to 12.5 micrometer aerodynamic diameter. For purposes of comparison, these quantitative tests with the PM_{10c} sampler were also conducted concurrently with a $PM_{2.5}$ FRM sampler and a total filter sampler.

This report will summarize results of the survey of analytical laboratories, describe procedures used during the qualitative and quantitative tests, and provide a summary of the study's results.

Survey of EDXRF Analytical Laboratories

Technical personnel were contacted at six analytical laboratories which routinely conduct EDXRF analysis of environmental samples: California Resources Board, Desert Research Institute, Oregon Department of Environmental Quality, RTI International, University of California at Davis, and the EPA's National Exposure Research Laboratory. As summarized in Table 1, this survey revealed that a variety of commercially available or custom made EDXRF instruments are used. Regardless of instrument design, however, these laboratories typically use an EDXRF beam size of either 10 mm or 20 mm equivalent diameter. These laboratories also typically analyze only the center of the filter and only one of the surveyed laboratories reported that the filter was rotated during the EDXRF analysis.

Personnel involved in post-sampling analysis of field filters reported occasionally observing a band of apparent higher deposition on the filter's outer deposition edge than was observed for the remainder of the filter. This band of apparent higher deposition was often more pronounced on one side of the filter than the other side. Opinions regarding the deposition pattern's source were varied and included particle bounce, filter and backing screen geometry, and flow leakage through the filter cassette. None of these

laboratory's surveyed personnel reported having conducted focused deposition uniformity tests nor were aware of uniformity studies involving use of $PM_{2.5}$, PM_{10c}, or PM_{10} FRM filters.

EXPERIMENTAL METHODS

Following the survey of the analytical laboratories, ORD conducted qualitative tests which involved stereoscopic examination of ambient aerosol samples collected during field sampling as well as examination of deposits obtained during sampling of laboratory generated aerosols. These qualitative tests were then followed by quantitative tests which were designed to determine the accuracy of using centrally located EDXRF spot sizes of 10 mm and 20 mm diameter to estimate the overall mass concentration of particles deposited over the entire filter surface.

Qualitative Test Procedures

For aerosol filter samples collected in the field and in the laboratory, visual observations were conducted using a variable magnification stereomicroscope (Model StereoZoom 5, Leica, Solms, Germany), which was equipped with ring-mounted illumination. Sizing of stereoscopic images was achieved using an optical micrometer which had been calibrated with a certified stage micrometer (American Optical, Model 1400, Southbridge, MA). Three-megapixel photomicrographs of stereoscope images were obtained using a DC3-SD digital camera (ESPA Systems, Jhubai City, Taiwan) in conjunction with MicroCap v2.0 imaging software.

Quantitative Test Procedures

Generation of Calibration Aerosols

Assessing the particle deposition uniformity of the FRM samplers involved use of calibration aerosols of known aerodynamic diameter, which is defined as the diameter of a unit density sphere which has the same settling velocity as the particle under consideration. In this study, separate uniformity tests were conducted using calibration aerosols of 0.035, 1.0, 2.5, 5.0, 10.0, and 12.5 micrometer aerodynamic diameter. For generation of the polydisperse aerosols with a mean diameter of 0.035 micrometers, a 6-jet nebulizer (Model 9306A, TSI Inc., Shoreview, MN) was operated at a gauge pressure of 25 psig in conjunction with use of a liquid solution of 1000 ppm volume concentration.

For generation of particles in the 1.0 to 12.5 micrometer size range, a Model 3050 (TSI Inc., Shoreview, MN) vibrating orifice aerosol generator (VOAG) was used to generate spherical particles of controllable diameter with known density. VOAG operation involves forcing a liquid solution through an orifice which is housed within a piezoelectric crystal. Monodisperse liquid droplets of known volume can then be produced by applying an AC signal to the crystal at a constant frequency. When the liquid solution consists to a non-volatile solute dissolved in a volatile solvent, the monodisperse droplets dry to form monodisperse particles of predictable diameter. Because the operating parameters of the VOAG (i.e., liquid flow rate, vibrational

frequency, solute concentration) can be controlled with minimal uncertainty, aerosols produced from the VOAG are considered to be a primary particle standard (John and Wall, 1983). Figure 1 is a schematic of the VOAG-based aerosol generation and sampling system used for determination of particle deposition uniformity in the FRM samplers.

Liquid flow was supplied to the VOAG using a dual-piston, digital HPLC pump (Model 1500, Lab Alliance, State College, PA) with a readability of 0.001 mL/min and an estimated uncertainty of 1%. Square-wave AC signals to the VOAG's piezoelectric crystal were supplied by a frequency generator (Model 3020, BK Precision, Yorba Linda, CA) with an estimated uncertainty of less than 0.1%. Applied vibrational frequencies were continuously monitored using a BK Precision Model 1803 frequency counter with a readability of 1 Hz.

All size selective tests conducted during this study employed the use of solid, spherical calibration aerosols composed of ammonium fluorescein. Liquid solutions of the desired volume concentrations were produced by dissolving a known mass of fluorescein powder (CAS 2321-073, J.T. Baker, Mallinckrodt, NJ) in a known volume of ammonium hydroxide. When generated under the proper conditions, ammonium fluorescein particles produced with the VOAG are smooth, spherical and possess a density of 1.35 g/cm^3 (Stober and Flacshbart, 1973; Vanderpool and Rubow, 1988).

Downstream of the aerosol generators, the generated droplets passed through a silica-gel based diffusion dryer (Model 3062, TSI Inc., Shoreview, MN) to facilitate drying of the generated droplets. The aerosol then entered a 0.03 m^3 stainless steel mixing chamber where the aerosol was mixed with dry dilution air. To verify the quality of generated aerosol, a sample of the dried calibration aerosol was periodically withdrawn at a flow rate of 16.7 Lpm and collected using a modified WINS impactor. For routine observations, aerosol samples were impacted on 25 mm x 55 mm rectangular glass slides coated with immersion oil. Following a two minute aerosol collection period, the glass slide was removed and a cover slip placed over the aerosol deposit. A drop of immersion oil was then placed on the cover slip and the particles observed at a magnification of 100X using a Nikon Labophot optical microscope (Nikon Inc., Melville, NY) to ensure that the generated particles were smooth and spherical. For purposes of documenting the size distribution and morphology of the generated aerosols, particles were alternatively impacted onto sticky carbon tape SEM stubs then examined using a Leica S440 scanning electron microscope (Leica Microsystems, Wetzlar, Germany). For collection of generated particles of aerodynamic diameter below the cutpoint of the WINS impactor, samples were collected on 46.2 mm diameter PTFE filters (Cat. 7592-104, Whatman Inc., Florham Park, NJ). Representatives sections of the filters were then removed and prepared for analysis by optical or scanning electron microscopy. SEM photomicrographs in Figure 2 illustrate the quality and uniformity of 5 µm diameter ammonium fluorescein particles generated using the VOAG during this study.

In addition to assessing the generated aerosol using microscopy, representative aerosol samples were continuously analyzed using a time-of-flight aerodynamic particle sizer (Model 3321 APS, TSI Inc., Shoreview, MN). In addition to validating the mean size of the particles generated by the VOAG, the APS was also valuable for ensuring that the VOAG's operation was stable and was not experiencing operational problems (e.g., orifice plugging, multiplet generation, satellite generation).

Once the quality of the generated aerosol was verified, the aerosol was introduced into a 20 mCi ^{85}Kr radioactive source (Model 3054A, TSI Inc., Shoreview, MN) in order to remove excess electrical charge which can be present on particles generated by the VOAG or the 6-jet nebulizer. The neutralized aerosol was then available for use in determining particle deposition uniformity in the FRM samplers. During these tests, no difference in the response of the APS was observed when sizing charged versus uncharged aerosols.

Aerosol Sampling

Aerosols which exited the charge neutralizer were introduced into a custom aerosol distribution manifold which was designed and constructed to uniformly distribute the calibration aerosol equally among the manifold's three outlets. Downstream of the manifold, each of the three sampling legs of the distribution manifold was of identical geometry and operated a volumetric flow rate of 16.7 Lpm. Separate tests conducted with 1 μm and 10 μm aerodynamic diameter particles revealed that the calibration aerosol was distributed uniformly among the three separate legs within 1% of the mean concentration. The use of large-bore, quarter-turn valves throughout the aerosol generation was designed to minimize particle transport losses. All components of the aerosol transport system downstream of the mixing chamber used tubing of 7/8" (2.2 cm) internal diameter and were composed of stainless steel to minimize corrosion. Components of the aerosol transport and sampling system were fabricated from electrically conductive materials and were grounded to minimize electrostatic particle losses.

As depicted in the Figure 1 schematic, the sampling system allowed direct introduction of calibration aerosols into the inlets of the WINS $PM_{2.5}$ fractionator and the total aerosol sampler. For introduction of aerosols into the PM_{10c} sampler, the louvered portion of the sampler was removed and a custom plenum attached and sealed to the remainder of the inlet. Figure 3 is a photograph of the PM_{10c} FRM sampler in this configuration.

Volumetric flow rate through the WINS fractionator (Cat. 57-004006, Thermo-Fisher, Waltham, MA) and its custom downstream filter holder was provided by a Thermo-Fisher Model 2000 FRM sampler. Volumetric flow rate through the Total Filter sampler was supplied by a BGI PQ200 FRM sampler (BGI Inc., Waltham, MA). The PM_{10c} sampler used for these tests was a designated Thermo-Fisher Model 2000 FRM sampler.

Calibrations of sampler flow rates, ambient temperature measurement, and ambient pressure measurement were conducted using an NIST-traceable calibration system (Model TetraCal, BGI Inc., Waltham, MA). Validation of the TetraCal's performance was conducted by EPA's APPCD Metrology Laboratory located in RTP, NC, using a Mobloc flow system (DH Instruments, Everett, WA). During the course of this study, the Mobloc was certified as having a combined uncertainty of ±0.3% of reading including uncertainties associated with measurement repeatability and hysteresis. The Metrology Laboratory's calibration of the TetraCal revealed that the TetraCal had an ambient temperature and pressure measurement bias of -0.4 C and -1 torr at measured conditions of 22.6 C and 757 torr, respectively. Flow calibration of the TetraCal revealed

that it had flow biases of 1.5%, -0.1%, and -0.3% at flow rates of 1.67 Lpm, 15.0 Lpm, and 16.7 Lpm, respectively.

Prior to the collection phase of the laboratory experiment, each of the three aerosol samplers was allowed to warm up for 15 minutes while sampling filtered air. The test aerosol was then introduced into the aerosol distribution manifold and the three samplers operated in parallel. Sampling run times varied from 3 minutes to 45 minutes per test, depending upon the expected mass concentration of the generated aerosol.

Following collection of laboratory generated calibration aerosols, the Teflon filter was removed from its sampler and inserted between two glass fiber filters (Cat. No. 66258, Pall Corp., Ann Arbor, MI). The filter stack was then positioned within a custom alignment assembly and the center portion of the stack was removed using either a 10 mm or a 20 mm nominal diameter punch composed of chrome vanadium steel (Mayhew Tools, Turners Falls, MA). The actual measured diameter of the two punches was measured to be 9.93 mm and 19.79 mm, respectively. The upper-most portion of the punched section was then removed for later extraction and fluorometric analysis. The remaining portion of the punched section was then inserted into a 2.5 cm x 5 cm folded section of 10 mesh stainless steel screen then the assembly was secured with stainless steel clips. This technique was developed to prevent the Teflon filter from collapsing into a ball which was found to prevent efficient recovery of the collected particles. The stainless steel filter assembly was then combined with the upper portion of the filter stack and placed into a 500 mL capacity polypropylene container. The same filter handling procedure was used for the section of the filter which remained after the punched section was removed. Extraction volumes of 0.01 N NH_4OH ranged from 50 mL to 1100 mL, depending upon the mass of collected calibration aerosols. Figure 4 is a photograph of punched glass fiber filters using various punch sizes.

To account for inadvertent particle losses to the steel punches, the outer and inner edges of each punch were each rinsed separately with approximately 10 mL of 0.01 N NH_4OH using a squeeze bottle and the extracts analyzed separately. Particle losses to the punch's inner and outer surfaces were then assumed to be associated with the inner and outer portions of the punched filter, respectively. As will be discussed, total losses to the punches were determined to be less than 0.1% by mass during all tests.

Sample Analysis

Deposits of ammonium fluorescein calibration aerosols were quantified using a Turner Quantech fluorometer (Model FM109515, Barnstead International, Dubuque, IA) equipped with NB490 and SC515 excitation and emission filters, respectively. Based on results from sensitivity tests of fluorescence intensity versus extraction solution pH (Tolocka et al., 2001), an ammonium hydroxide solvent concentration of 0.01 N was selected for all extractions conducted during this study. Calibration standards for the fluorometer were prepared by dissolving a known mass of fluorescein powder in ammonium hydroxide, and all fluorometric measurements were made in the fluorometer's linear range of 0 to 200 ng/mL.

Filter background tests were conducted by placing 46.2 mm diameter PTFE filters in 125 mL capacity polypropylene jars containing 10 mL of 0.01 N NH_4OH. The jars were then placed in an ultrasonic bath for 1 hr and the extracts analyzed. Replicate tests

showed that the background content of the Whatman filters was below the 0.31 ng/mL detection limit of the analytical technique (i.e., 3.1 ng for this extraction volume). Similar background results were obtained for the two steel punches used in the study.

Extraction efficiency tests were conducted by delivering 0.1 mL of a 10,000 ng/mL fluorescein standard to the PTFE filters and allowing the filters to air dry. The filters were then extracted in the same manner as during the background tests. Results showed that the extraction efficiencies for the 46.2 mm filters used in these tests exceeded 98%. Notably, the same extraction efficiency was achieved by sealing the container, allowing a 30 equilibration time, then vigorously shaking the container for 2 minutes. This result indicated that the ammonium fluorescein readily dissolved in the 0.01 N NH_4OH solution, thus avoiding the need to sonicate collected aerosol deposits during the study.

DATA ANALYSIS

If MF_i and MF_o represent the measured aerosol mass on in the inner and outer portions of the punched filter, respectively, and MP_i and MP_o represent the measured aerosol mass on the punch's inner and outer wall, respectively, then the total mass (M_t) on the filter can be calculated as:

$$M_t = (MF_i + MP_i) + (MF_0 + MP_o)$$

and the fractional loss of mass to the punch can be calculated as:

$$Punch\ Loss = \frac{(MP_i + MP_o)}{M_t}$$

If A_i and A_t represent the area of the punch and the total filter deposition area, respectively, then the accuracy of using a centrally located punch can be calculated as the filter's estimated aerosol mass divided by the filter's actual aerosol mass:

$$Accuracy\ Ratio = \frac{Estimated\ Mass}{Actual\ Mass} = \frac{(MF_i + MP_i)}{M_t} * \left(\frac{A_t}{A_i}\right)$$

For a filter with a perfectly uniform deposition pattern, the estimated mass based on analysis of the punch would be identical to the actual mass (i.e., accuracy ratio = 1.000)

RESULTS

Qualitative Analysis of Collected Field Filters

Qualitative analysis first involved the stereoscopic inspection of field from a variety of sources including ORD's previous field studies in Riverside, CA and

Birmingham, AL, as well samples submitted by Oregon's Department of Environmental Quality (ODEQ).

Figure 5 shows stereomicrographs of a $PM_{2.5}$ filter collected by ODEQ showing the basic structure of the 46.2 mm PTFE filters and the deposition pattern of aerosols collected during this sampling event. As the two photomicrographs show, there exists a thin band of aerosol deposits at the outer edge of the filter membrane which differs in appearance from the remainder of the filter. For this particular filter, the deposition band is present around the entire circumference of the filter. The deposition pattern on the interior portion of the filter is consistent with the pattern of holes in the underlying backing screen. Personnel at ODEQ report that this deposition band is present on PM_{10} FRM samplers and speciation samplers which use this same cassette and PTFE filter.

From inspection of a different $PM_{2.5}$ filter provided by ODEQ, the stereomicrographs presented in Figure 6 illustrate that the deposition band is not always uniformly present around the filter's entire circumference. The absence of the deposition band is also demonstrated in Figure 7 for a filter collected by EPA's ORD during field sampling in Birmingham, AL. Following inspection of several dozen filters collected from multiple ORD field studies, it was observed that the deposition band was always present to some degree and was most visible of filters which were lightly to moderately loaded. Similar to the pattern depicted in Figure 6, it was also observed that the deposition band was often more prominent on one side of the filter and often completely absent on the other side of the filter. The size of the deposition band typically varied from one filter to another and averaged approximately 0.5 mm in width.

In order to determine whether the pattern of apparently high loading was due to higher air flow in the region of the deposition band, a high-contrast sub-micrometer aerosol was generated in the laboratory using dark green food coloring. Because the sub-micrometer particles produced from air nebulization of this low-concentration fluid tend to follow fluid streamlines very closely, the deposition produced from this aerosol provides an accurate measure of the air flow pattern. As depicted in Figure 8, the deposition band produced in laboratory was very similar in appearance to the deposition bands produced during field sampling. Figure 9 provides an image of the underlying backing screen next to an image of this filter and illustrates that the deposition band can form even when the screen's holes are located directly underneath the band's formation region.

In the laboratory, it was determined that the Whatman PTFE filters met all the required dimensional and performance specifications for FRM filters with regard to filter diameter, width and thickness of the polypropylene support ring, filter membrane thickness, and pressure drop. A series of leak check tests revealed that no air flow leaks were occurring around or through the edge of the filter. Further, it was determined that the deposition band did not form in the laboratory when glass fiber filters or cellulose filters were substituted for the PTFE filters. It was thus concluded that formation of the deposition band was a function of the design the PTFE filters themselves rather due to the geometry of the filter cassette or the flow pattern immediately upstream of the cassette.

The filter cassette assembly for an FRM filter is illustrated in Figure 10 and consists of a cassette upper housing, cassette lower housing, backing screen, and PTFE filter. All dimensional and performance specifications for these components are provided in 40 CFR Part 50 Appendix L (U.S. EPA, 1997). A close-up of the cassette assembly in

Figure 11 illustrates the geometry of the Teflon filter in relation to the lower cassette and the backing screen. As specified in the regulations, the Teflon filter consists of a thin Teflon fiber membrane whose outside edge is supported by a polypropylene support ring. The purpose of the support ring is to provide dimensional stability to the Teflon membrane and to provide an airtight seal without damage to the membrane. Because the 40 micrometer thick Teflon membrane is affixed within the center of the 365 micrometer thick support ring, the outside edge of the filter membrane is suspended approximately 160 micrometers above the backing screen.

At the 16.7 Lpm flow rate though the cassette assembly during sampling, the pressure drop through the Teflon filter is approximately 15 torr. This relatively high flow resistance forces the majority of the Teflon membrane against the upper surface of the backing screen. In this region, flow through the filter is constrained to only those areas immediately above the holes in the perforated backing screen and accounts for the deposition pattern observed in Figures 5 though 9. However, at the extreme outside edge of the filter membrane, the filter remains suspended above the backing screen. Because flow in this region is not constrained by the geometry of the backing screen, a different airflow pattern results in this region. It was thus conjectured that this difference in airflow pattern was the mechanism for formation of the deposition band around the Teflon surfaces. The conjecture is supported by the prior tests showing that no deposition band forms around either glass fiber filters or quartz filters. Unlike the FRM's Teflon filters, neither the glass fiber filters nor the quartz filters have a support ring.

Per the cassette assembly's design specifications, the internal diameter of the cassette lower housing is 47.0 mm, while the outside diameter of the backing screen and the Teflon filter are nominally 46.6 mm and 46.2 mm, respectively. These specifications were designed to allow for some tolerance in the manufacture of the components and to ensure that the edges of the filter and backing screen would not bind and chafe when installed in the cassette. This difference in dimensions allows some side-to-side displacement of the filter and backing screen relative to each other and affects the location of the deposition band. If the cassette's lower housing, filter, and backing screen are all concentrically aligned during assembly (as in Figure 12), then the deposition band of equal width will be formed around the entire outer edge of filter. If, however, the filter and screen are shifted from a concentrically aligned position, then the deposition pattern will not be uniform around the filter's edge. Figures 13 and 14 depict the left and right sides of a cassette assembly where the filter is shifted completely to the left while the backing screen is shifted completely to the right. In this instance, the deposition band would be completely absent on the left side of the filter but present on the right side of the filter.

The deposition band could be completed eliminated if the backing screen was redesigned to have a smaller deposition diameter. Figure 15 shows the absence of deposition formation which resulted from laboratory testing of a prototype of this redesigned screen.

Quantitative Analysis of Laboratory Filters

Qualitative tests confirmed previous visual observations that a deposition band forms at the outside edge of FRM filters. However, the calculated area of this deposition

band typically represents only about 5% of the filter's total deposition area. Moreover, the qualitative tests could not determine the relative influence of the deposition band on the filter's overall degree of uniformity. Quantitative tests in the laboratory were thus required to determine if the deposition band adversely affected the accuracy of using centrally located punches to estimate overall deposited aerosol mass.

10 mm Punch Results

As mentioned, particles losses to the chrome vanadium steel punches were quantified during the laboratory experiments. Results for the 10 mm punches revealed that particle losses were negligible, as indicated by mean loss of 0.034%. For all samplers and particle sizes tested, the mass loss to the 10 mm steel punch during a single analysis did not exceed 0.07%.

Table 2 summarizes results of the laboratory tests to determine the accuracy of using a centrally located 10 mm diameter punch to estimate the actual concentration over the filter's entire deposition area. As previously mentioned, tests were first conducted with polydisperse aerosols of 0.035 micrometers diameter because these submicrometer aerosols serve as efficient flow tracers. Despite the formation of the deposition ring (Figure 8), quantitative results indicated that the adverse influence of the deposition band was negligible. For the $PM_{2.5}$, PM_{10c}, and PMtotal sampler, the estimated to actual concentration ratio for the 0.035 micrometer aerosol was determined to be 0.981, 1.004, and 0.979, respectively, for a mean value of 0.988.

For all particle sizes tested, inspection of Table 2 reveals that the lowest ratio was measured to be 0.943 while the highest ratio was measured to be 1.021. No appreciable difference in test results was observed as a function of particle size nor as a function of sampler type. For all sizes tested, the mean ratios for the $PM_{2.5}$, PM_{10c}, and PMtotal samplers was determined to be 0.981, 0.994, and 0.982, respectively. Averaging all particle size data among the three sampler types produced a mean estimated to actual concentration ratio of 0.988. Despite the fact that a 10 mm punch represents only 6.6% of the total deposition area, these tests demonstrate that the area is quantitatively representative of the entire deposition area.

20 mm Punch Results

Particle mass losses to the 20 mm diameter punch were similar to those of the 10 mm punch, as indicated by a mean value of 0.030%. For all samplers and particle sizes tested, the mass loss during a single analysis did not exceed 0.09%.

As summarized in Table 3, results obtained using the 20 mm diameter punch were similar to those obtained with the 10 mm punch. For the 0.035 micrometer polydisperse aerosols, the estimated to actual concentration ratio for the $PM_{2.5}$, PM_{10c}, and PMtotal sampler was determined to be 0.993, 1.014, and 0.994, respectively, for a mean value of 1.000. For all sizes tested, the mean ratios for the $PM_{2.5}$, PM_{10c}, and PMtotal samplers was determined to be 0.972, 0.993, and 0.985, respectively. Averaging all particle size data among the three sampler types produced a mean estimated to actual concentration ratio of 0.986.

To determine the degree of variability associated the quantitation procedure, three replicate tests were performed using 10 micrometer aerosols as sampled by the PM_{10c} sampler. Values of estimated to actual mass ratios for the three replicate tests were 0.970, 0.993, and 1.004, resulting in a standard deviation of 1.7%.

SUMMARY AND CONCLUSIONS

1. EPA's proposed revisions to the NAAQS for Pb involves EDXRF analysis of Teflon filters collected with designated PM_{10c} FRM samplers. Because EDXRF analysis only analyzes approximately 7% to 26% of the filter's deposition area, measurement biases would result if Pb-based particles were not deposited on the filter in a spatially uniform manner. The purpose of this study was to quantify the degree of spatial uniformity of particles on PM_{10c} FRM filters. For purposes of comparison, similar tests were conducted with a $PM_{2.5}$ FRM sampler and a total filter sampler.

2. A survey of EDXRF analytical laboratories revealed that incident beam spot sizes of 10 mm and 20 mm diameter are typical and that the incident beams are typically positioned at the center of 47 mm diameter filters.

3. Qualitative analysis involved stereoscopic examination of FRM filters collected in the field from a variety of sources, as well as examination of filters collected using laboratory generated calibration aerosols. Results confirmed anecdotal reports of the presence of a region of apparently higher deposition at the filter's outer edge than existed for the remainder of the filter. Independent of particle size or sampler type, similar results were observed following collection of laboratory generated aerosols. Formation of the deposition band occurred only with the FRM's Teflon filters and did not occur in the laboratory using either glass fiber filters or quartz filters. Subsequent tests identified that the formation of the deposition band resulted from the outside edge of the filter membrane being suspended approximately 0.16 mm above the underlying backing screen due to the filter's support ring geometry. This mechanism also explained why the deposition band was not always uniformly present around the filter's circumference. Tests with a prototype backing screen design revealed that the deposition band could be eliminated by a slight reduction in the diameter of the screen's perforated area.

4. Quantitative tests involved the generation of fluorometric calibration aerosols in six discrete sizes from 0.035 micrometers to 12.5 micrometers aerodynamic diameter. Samples of the generated aerosols were concurrently obtained by a $PM_{2.5}$ FRM sampler, a PM_{10c} FRM sampler, and a PMtotal sampler which consisted only of a FRM filter holder. 10 mm and 20 mm diameter chrome vanadium steel punches were used to remove sections from the filters, and aerosol mass deposits were quantified fluorometrically.

5. Laboratory test results indicated that either a 10 mm or 20 mm centrally located spot provides an accurate estimate of the filter's overall mass concentration within approximately 2%. These results were found to be independent of particle size or sampler type. For all particles sizes tested, use of a 10 mm punch resulted in mean estimated to actual concentration ratios for the $PM_{2.5}$, PM_{10c}, and PMtotal samplers of 0.972, 0.993, and 0.985, respectively. For the 20 mm diameter punch, the mean estimated to actual concentration ratios for the $PM_{2.5}$, PM_{10c}, and PMtotal samplers was determined to be 0.972, 0.993, and 0.985, respectively. With particular relevance to the proposed revisions the Pb NAAQS, use of the 10 mm and 20 mm punches with filters collected with the PM_{10c} sampler resulted in mean estimated to actual ratios of 0.994 and 0.993, respectively.

6. Based on the results of these qualitative and quantitative tests, it can be concluded that the magnitude of non-uniform particle deposition on FRM filters is relatively minor. Non-uniformity thus represents a negligible fraction of the overall uncertainty in Pb compliance measurements involving the proposed use of EDXRF analysis of filters collected using a PM_{10c} FRM sampler.

REFERENCES

John, W.; Wall; S.M. Aerosol Testing Techniques for Size-Selective Samplers; *J. Aerosol Sci.* **1983**, 14(6): 713-727.

Stober, W.; Flacshbart, H. An Evaluation of Nebulized Ammonium Fluorescein as a Laboratory Aerosol; *Atmos. Env*., **1973**, 7: 737-748.

Tolocka, M.P.; Tseng, P.T.; Wiener, R.W. Optimization of the Wash-Off Method for Measuring Aerosol Concentrations; *Aerosol Sci. Technol*. **2001**, 34: 416-421.

U.S. Environmental Protection Agency, 40 CFR Subpart 50 Appendix L; *Fed. Regist.* **1997**, 62.

Vanderpool, R.W.; Rubow, K.L. Generation of Large, Solid Monodisperse Calibration Aerosols; *Aerosol Sci. Technol.*, **1988**, 9: 65-69.

ACKNOWLEDGEMENTS

The authors gratefully acknowledge the useful discussions with Bob Kellogg of Alion Science and Technology, and Ben Jones of Oregon's Department of Environmental Quality.

Table 1. EDXRF instruments and setup conditions reported by the surveyed analytical laboratories.

Analytical Laboratory	EDXRF Instrument	Equivalent Beam Diameter (mm)	Beam Location	Sample Rotated During Analysis?
California Air Resources Board (CARB)	Thermo QuanX	20	Centered	Yes
Desert Research Institute (DRI)	PanAnalytical Epsilon 6	20	Centered	No
Oregon Department of Environmental Quality (ODEQ)	Kevex 771	10	Centered	No
RTI International	Thermo QuanX	20	Centered	No
University of California at Davis (UCD)	UCS design and build	9.4	Centered	No
EPA National Exposure Research Laboratory	Lawrence Berkeley Laboratory (LBL) 1984 design and build	20	Centered on a 37 mm filter, approx. 5 mm off-center on a 47 mm filter	No

Table 2. Ratio of estimated concentration to actual concentration as a function of aerodynamic diameter and sampler. Punch diameter = 10 mm

Aerodynamic Diameter (µm)	(Estimated Concentration)/(Actual Concentration)			
	Sampler			
	$PM_{2.5}$ FRM	PM_{10c} FRM	PMtotal	Mean
0.035	0.981	1.004	0.979	0.988
1.0	0.984	0.963	0.943	0.963
2.5	0.977	0.988	1.012	0.992
5.0	-	1.021	0.980	1.001
10.0	-	0.992	0.989	0.991
12.5	-	0.999	0.990	0.995
Mean	**0.981**	**0.994**	**0.982**	**0.988**

Table 3. Ratio of estimated concentration to actual concentration as a function of aerodynamic diameter and sampler. Punch diameter = 20 mm

Aerodynamic Diameter (µm)	(Estimated Concentration)/(Actual Concentration)			
	Sampler			
	$PM_{2.5}$ FRM	PM_{10c} FRM	PMtotal	Mean
0.035	0.993	1.014	0.994	1.000
1.0	0.933	0.993	0.959	0.962
2.5	0.990	0.974	0.990	0.985
5.0	-	0.981	0.973	0.977
10.0	-	0.989	0.993	0.991
12.5	-	1.012	0.988	1.000
Mean	**0.972**	**0.993**	**0.985**	**0.986**

Note: Perfectly uniform deposition would result in estimated/actual ratios equal to 1.000

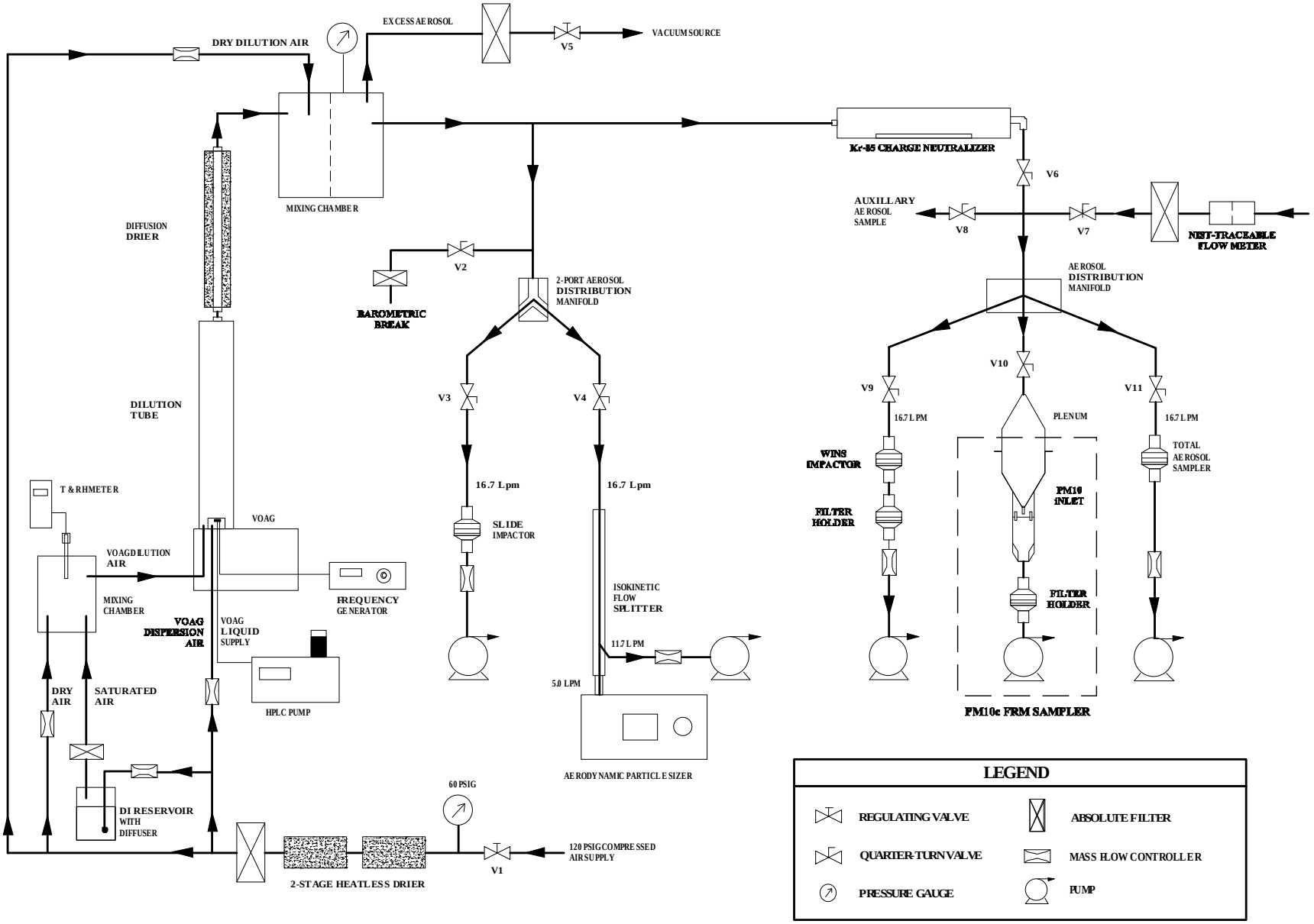

Figure 1. Schematic of the aerosol generation and sampling system used for determination of particle deposition uniformity. For generation of the 0.035 micrometer particles, the VOAG generator was replaced with a 6-jet nebulizer.

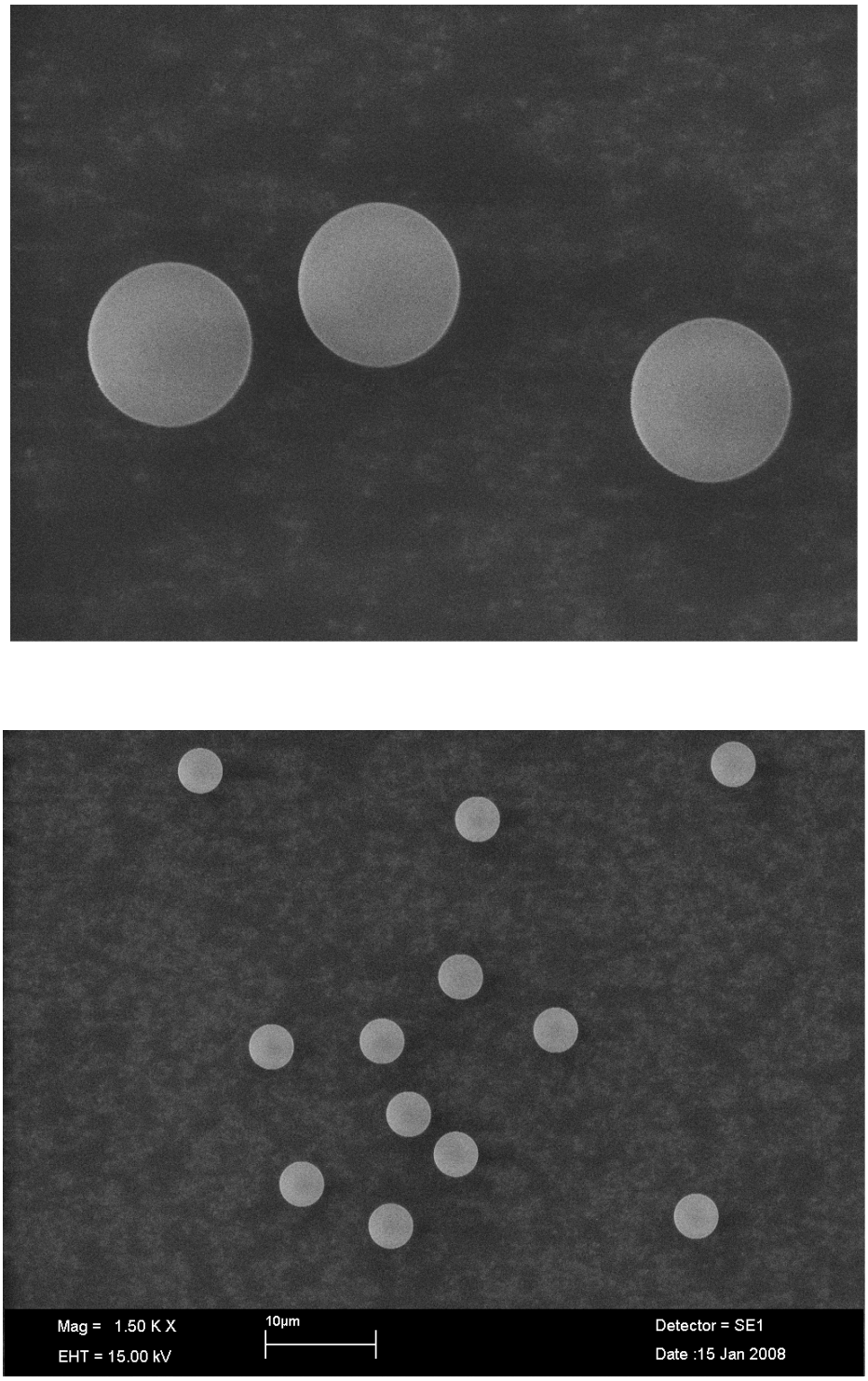

Figure 2. SEM photomicrographs of 5 micrometer ammonium fluorescein calibration aerosols showing the particles' quality and size uniformity. The upper and lower photomicrographs were obtained at SEM magnifications of 5,000X and 1,500X, respectively.

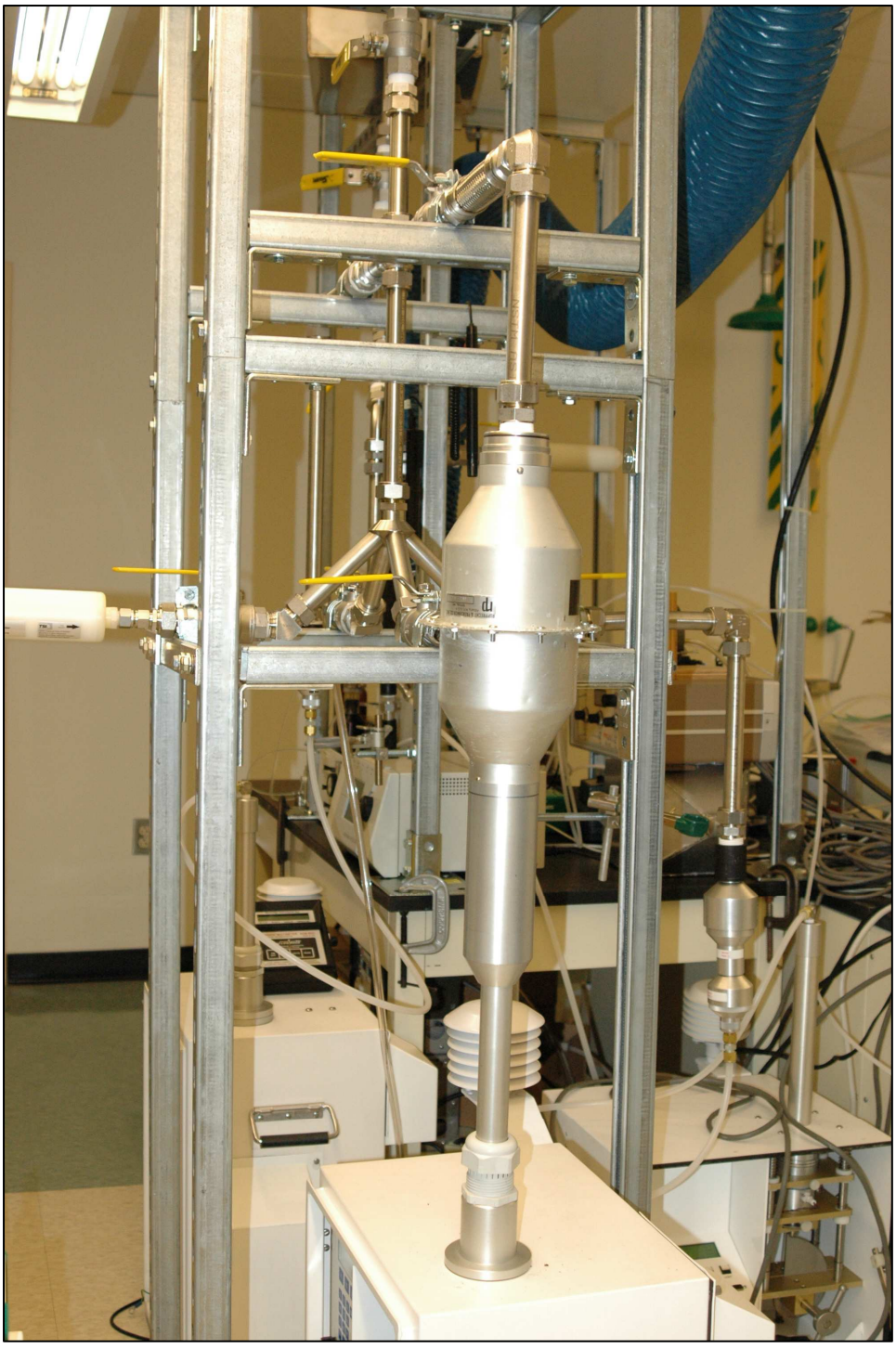

Figure 3. Photograph of the aerosol sampling system showing the plenum used for introducing calibration aerosols into the PM_{10c} sampler.

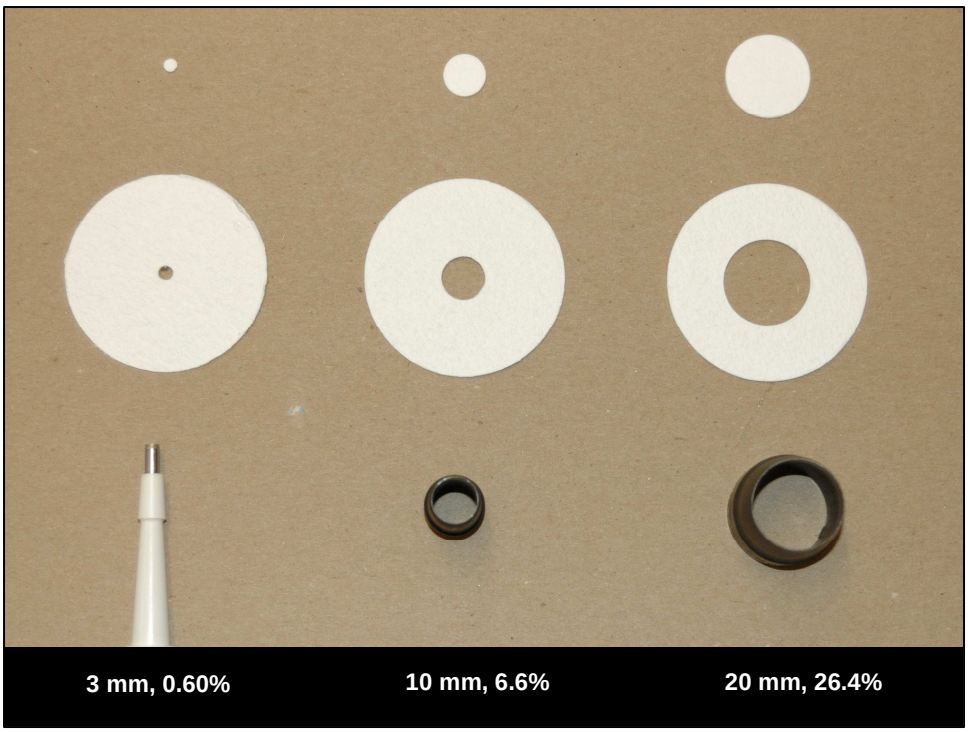

Figure 4. Photograph of inner and outer portions of punched filters as a function of punch diameter. The punch diameter and the percent area that the punch represents are listed below each filter. The 3 mm diameter punch area is similar to the beam size used for particle induced X-ray elemental (PIXE) analysis.

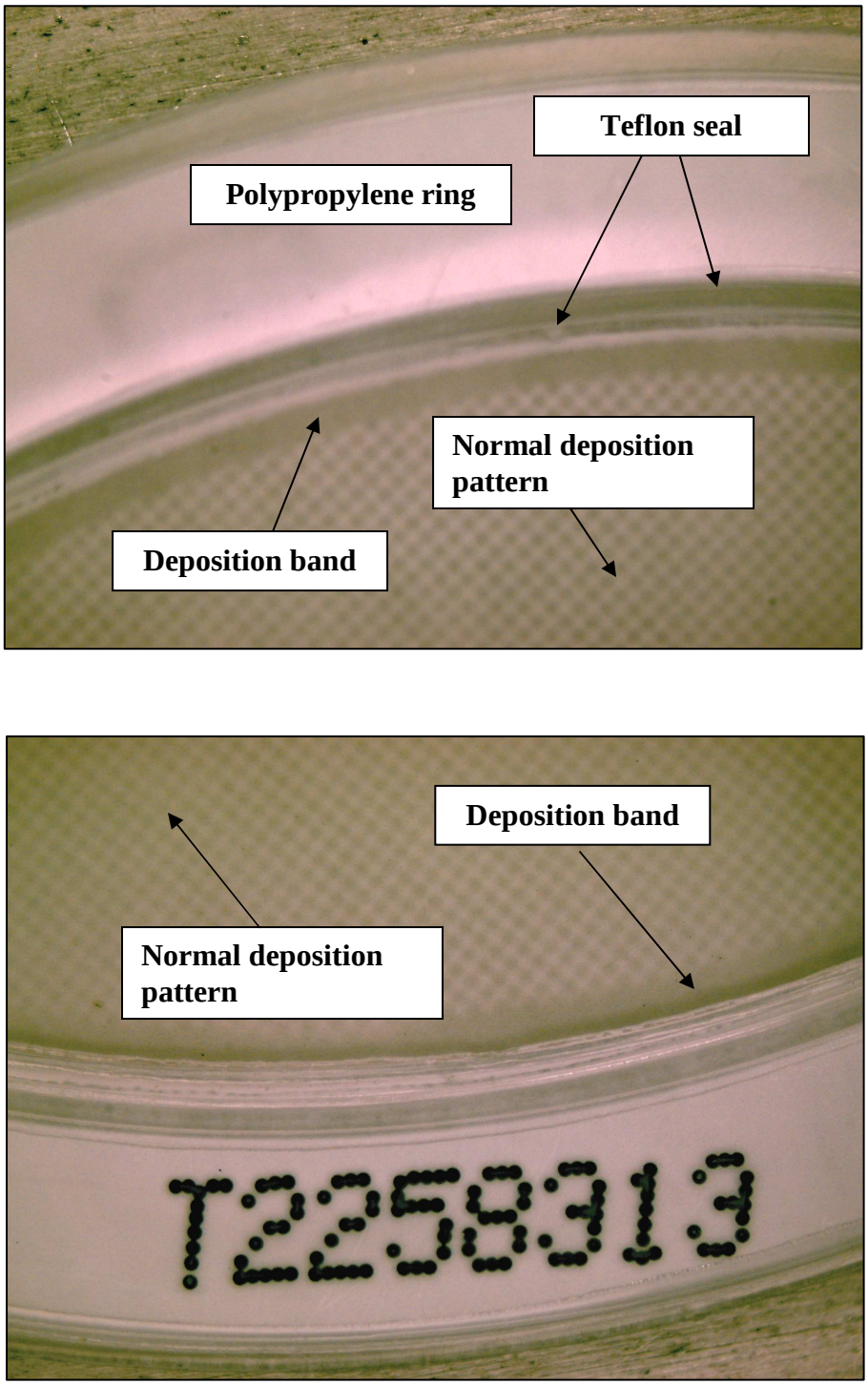

Figure 5. Stereomicrograph of a $PM_{2.5}$ field filter supplied by the Oregon DEQ. The deposition band is visible at the top and the bottom of the filter.

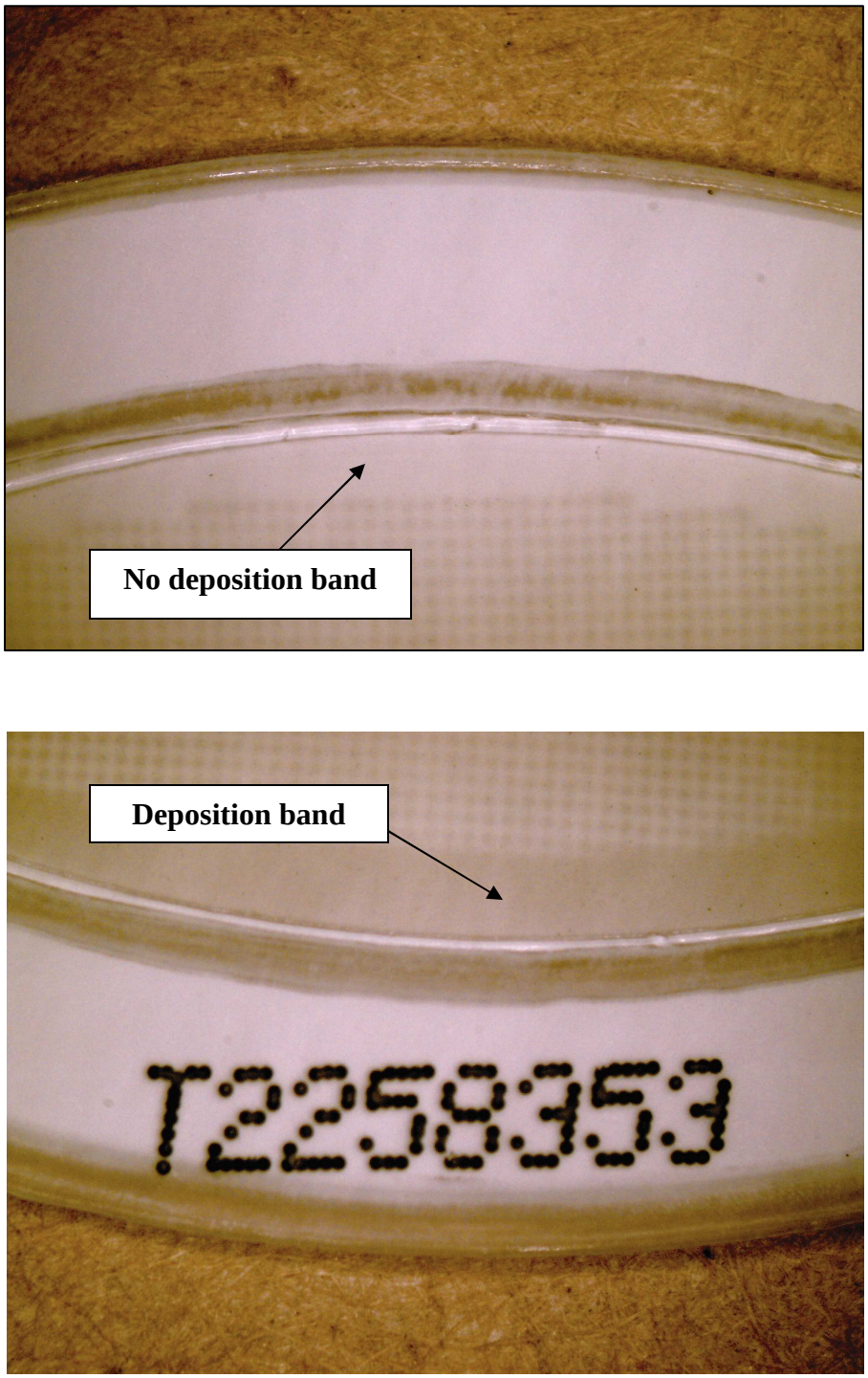

Figure 6. Stereomicrograph of field filter supplied by the Oregon DEQ. The deposition band is not present at the filter's top but is visible on the bottom of the filter.

Figure 7. Stereomicrograph of field filter collected by ORD during field sampling in Birmingham, AL. No deposition band formed at the bottom of this filter.

Figure 8. Stereomicrograph of submicron aerosol generated and collected in the laboratory. The submicron aerosol makes an efficient flow tracer and indicates higher flow at the filter's lower edge than at other portions of the filter.

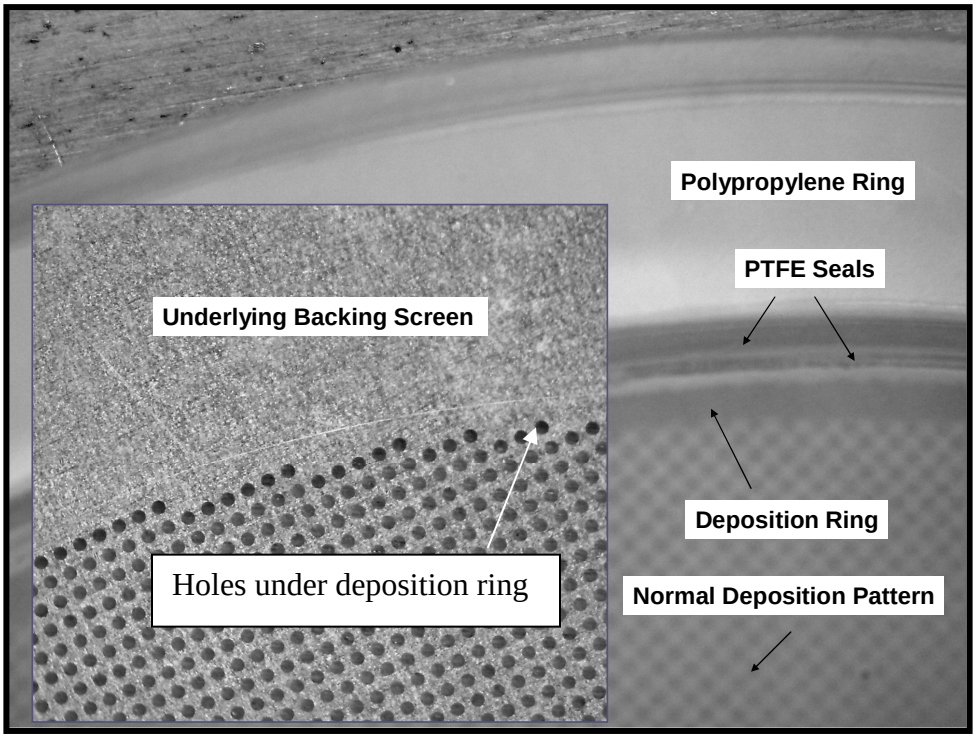

Figure 9. Stereomicrograph of submicron aerosol generated and collected in the laboratory. The superimposed image of the underlying backing screen indicates that the deposition ring forms at the outside edge even when holes are present.

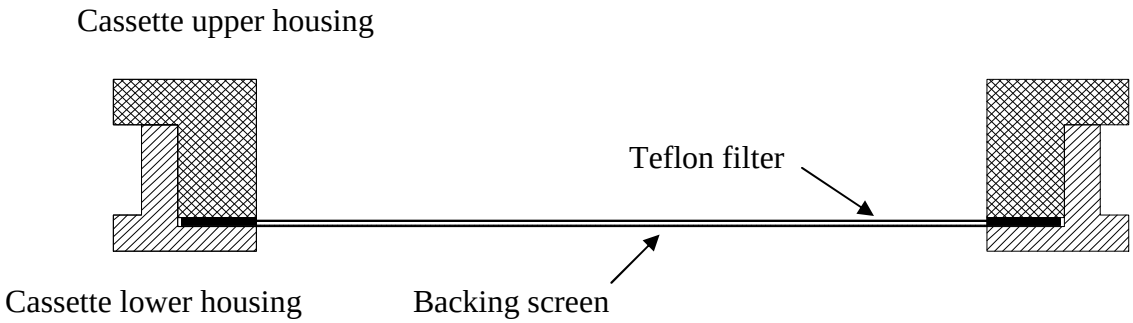

Figure 10. Cross sectional view of FRM cassette assembly showing components.

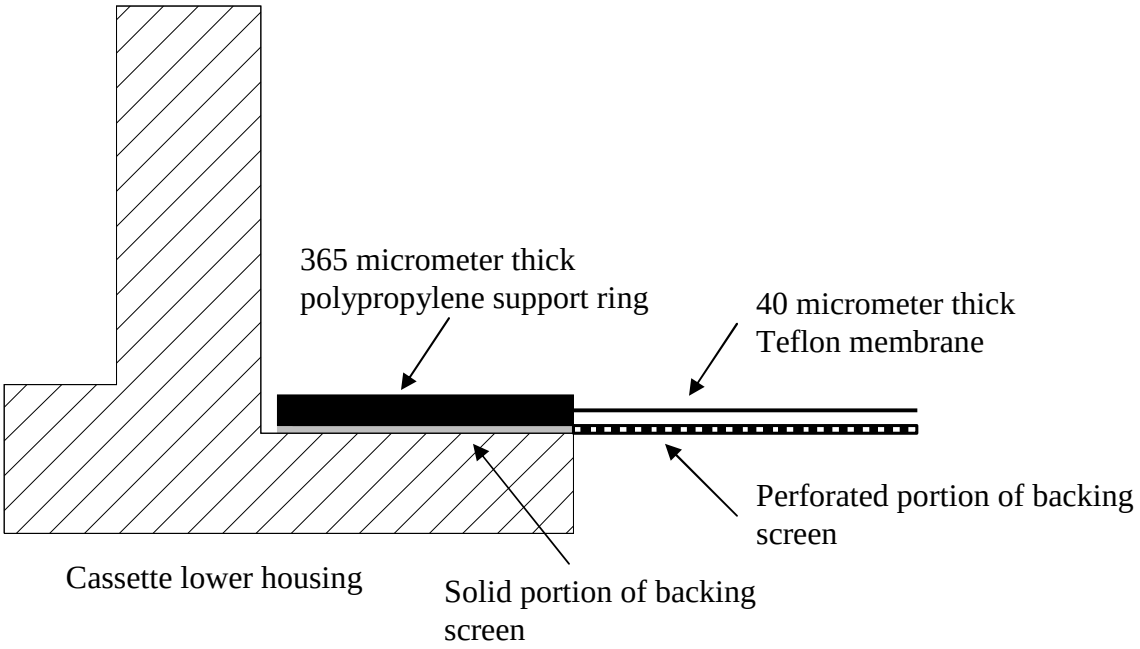

Figure 11. Close-up of the cassette assembly showing the geometry of the filter and backing screen in the absence of air flow. Note that the cassette's upper housing has been removed for purposes of clarity.

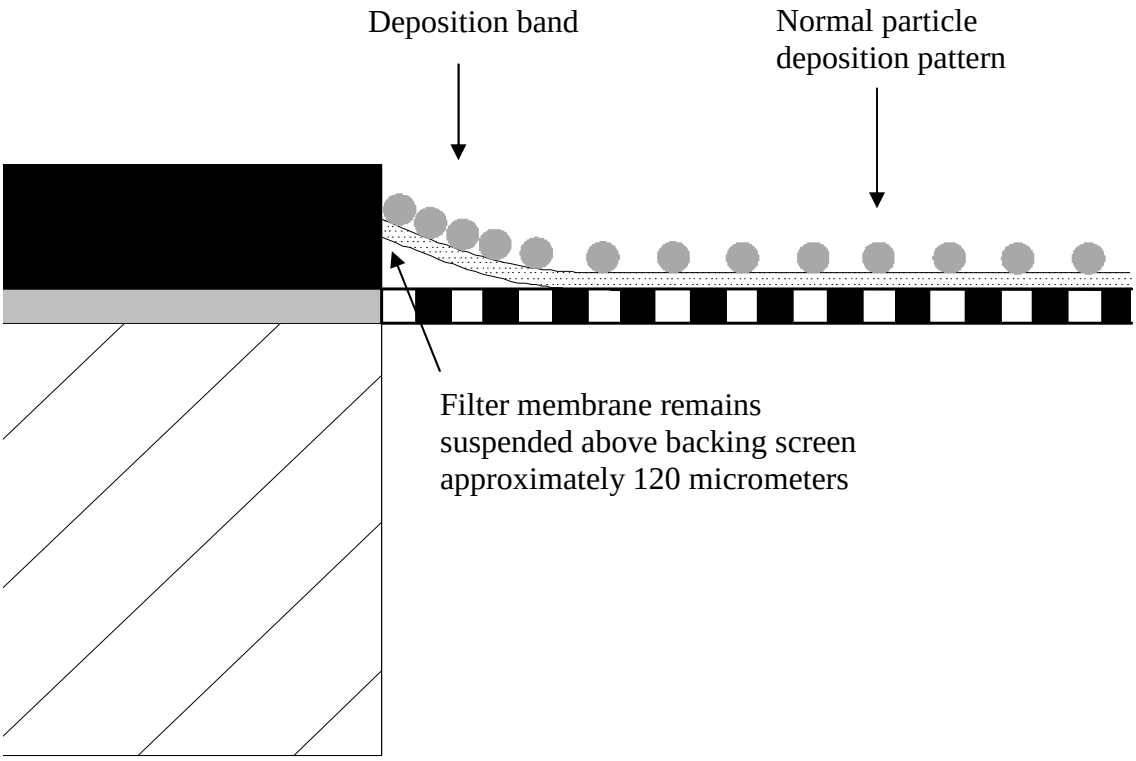

Figure 12. Close-up of cassette assembly showing mechanism of deposition band formation during aerosol sampling.

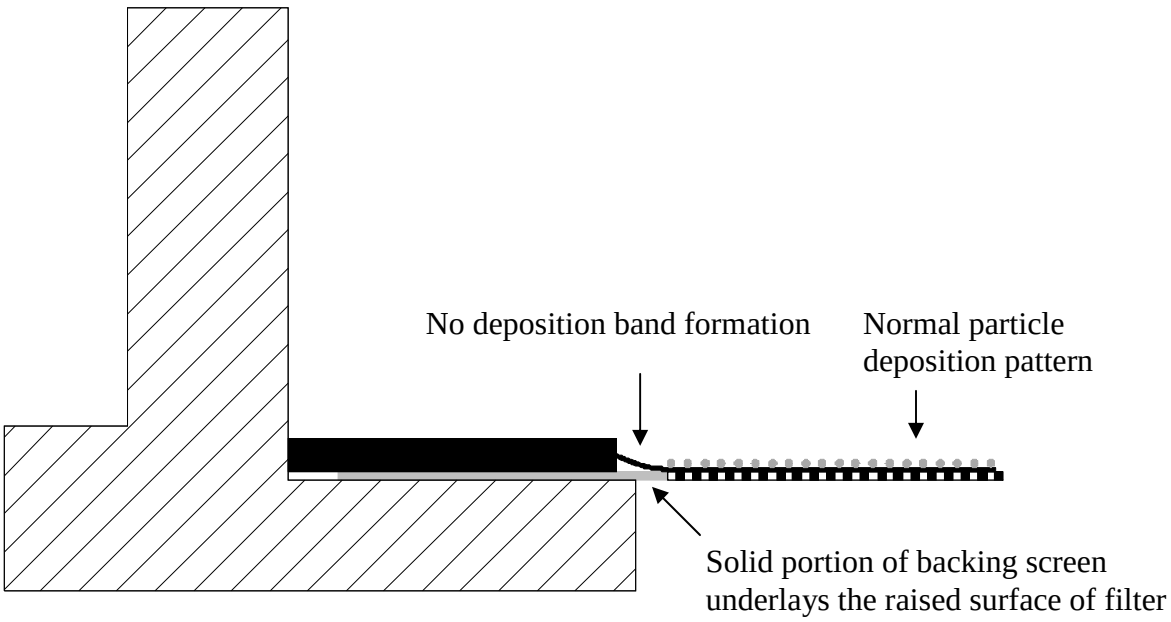

Figure 13. Close-up of left side of cassette assembly when filter and backing screen are shifted horizontally in opposite directions. No deposition band forms on the left side of the filter.

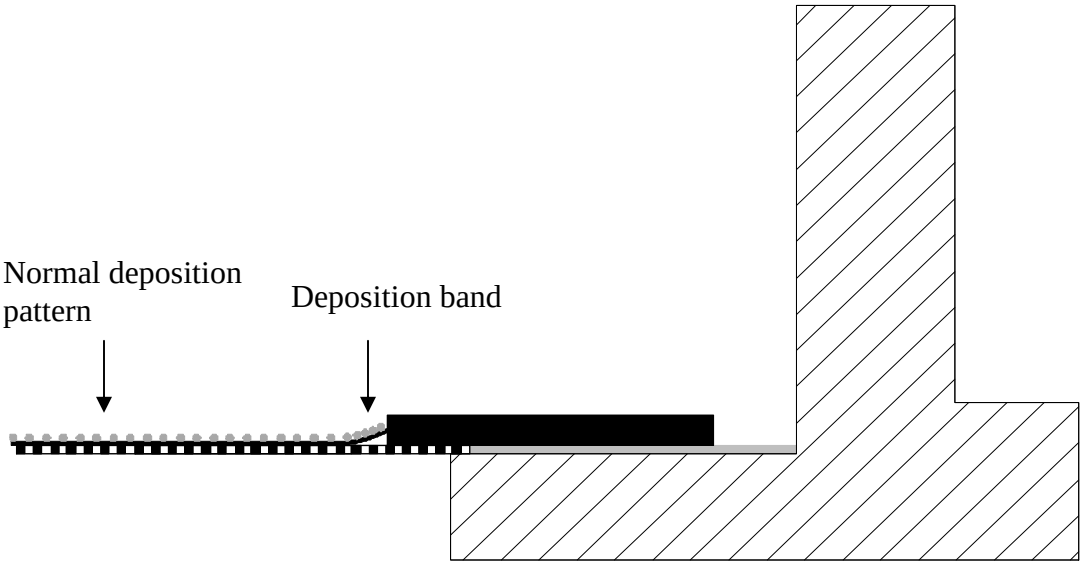

Figure 14. Close-up of right side of cassette when filter and backing screen are shifted horizontally in opposite directions. A deposition band forms on the right side of the filter.

Figure 15. Stereomicrograph showing deposition pattern using a redesigned backing screen. No deposition band formed at the filter's edge.